




Effects of Myeloid *Hif-1 β* Deletion on the Intestinal Microbiota in Mice under Environmental Hypoxia

Ni Han,^a Zhiyuan Pan,^a Zongyu Huang,^a Yuxiao Chang,^a Fengyi Hou,^a Guangwei Liu,^b Ruifu Yang,^a  Yujing Bi^a

^aState Key Laboratory of Pathogen and Biosecurity, Beijing Institute of Microbiology and Epidemiology, Beijing, China

^bKey Laboratory of Cell Proliferation and Regulation Biology of Ministry of Education, Institute of Cell Biology, College of Life Sciences, Beijing Normal University, Beijing, China

Ni Han and Zhiyuan Pan contributed equally to this article. Author order was determined both alphabetically and in order of increasing seniority.

ABSTRACT External environmental factors can cause an imbalance in intestinal flora. For people living in the extremes of a plateau climate, lack of oxygen is a primary health challenge that leads to a series of reactions. We wondered how intestinal microorganisms might change in a simulated plateau environment and what changes might occur in the host organism and intestinal microorganisms in the absence of hypoxia-related factors. In this study, mice carrying a knockout of hypoxia-inducible factor 1 β (*Hif-1 β*) in myeloid cells and wild-type mice were raised in a composite hypoxic chamber to simulate a plateau environment at 5,000 m of elevation for 14 days. The mice carrying the myeloid *Hif-1 β* deletion displayed aggravated hypoxic phenotypes in comparison to and significantly greater weight loss and significantly higher cardiac index values than the wild-type group. The levels of some cytokines increased in the hypoxic environment. Analysis of 16S rRNA sequencing results showed that hypoxia had a significant effect on the gut microbiota in both wild-type and *Hif-1 β* -deficient mice, especially on the first day. The levels of members of the *Bacteroidaceae* family increased continuously from day 1 to day 14 in *Hif-1 β* deletion mice, and they represented an obviously different group of bacteria at day 14 compared with the wild-type mice. Butyrate-producing bacteria, such as *Butyricoccus*, were found in wild-type mice only after 14 days in the hypoxic environment. In conclusion, hypoxia caused heart enlargement, greater weight loss, and obvious microbial imbalance in myeloid *Hif-1 β* -deficient mice. This study revealed genetic and microecological pathways for research on mechanisms of hypoxia.

KEYWORDS *Hif-1 β* , gut microbiota, imbalance, hypoxia, imbalance, myeloid cell

According to the international classification scale, 1,500 to 3,500 m above sea level is considered a high-altitude environment for human life; with enough time at this elevation, most people can adapt. At the very high altitude range of 3,500 to 5,500 m, physiological differences determine who can or cannot adapt; above 5,500 m of elevation, human bodily functions seriously decline, with some of the damage being irreversible (1–4). No human can survive at this height for a full year, and even native Tibetans and Sherpas generally live in areas with altitudes below 5,500 m (5). Altitude sickness is thought to mainly result from the body adapting to conditions at higher altitudes, such as cold temperatures, low oxygen levels, and strong radiation (6), which produce a series of natural physiological reactions. The harsh natural environment of the plateau lowers immunity and the ability to cope with special environments. It is easier to catch colds and develop gastrointestinal diseases, which can lead to gastrointestinal digestive dysfunction. Food intake, absorption, digestion, metabolism, and excretion are affected to differing degrees. When a person enters a high altitude, the

Citation Han N, Pan Z, Huang Z, Chang Y, Hou F, Liu G, Yang R, Bi Y. 2021. Effects of myeloid *Hif-1 β* deletion on the intestinal microbiota in mice under environmental hypoxia. *Infect Immun* 89:e00474-20. <https://doi.org/10.1128/IAI.00474-20>.

Editor Andreas J. Bäuml, University of California, Davis

Copyright © 2020 American Society for Microbiology. All Rights Reserved.

Address correspondence to Ruifu Yang, 13801034560@163.com, or Yujing Bi, byj7801@sina.com.

Received 29 July 2020

Accepted for modification 19 August 2020

Accepted 21 September 2020

Accepted manuscript posted online 26 October 2020

Published 15 December 2020

spinal cord quickly produces a large number of new red blood cells (RBCs) to improve the blood's ability to carry oxygen (7).

Studies have shown that the hypoxia-inducible factor 1 (HIF-1) pathway is actively expressed in a hypoxic environment (8). Transcription factors that are induced by HIFs during tissue hypoxia were first discovered in 1991 by Semenza et al., using electrophoretic displacement analysis of nuclear extracts from Hep3B and HepG2 cell lines exposed to hypoxia (9). In a low-oxygen environment, the body uses the HIF-1 pathway to relieve oxygen deficiency. HIF-1 is a transcription complex composed of a 120-kDa α subunit and an approximately 91-to-94-kDa β subunit. The α subunit, HIF-1 α , is actively regulated by oxygen levels. HIF-1 β (also known as aryl hydrocarbon receptor nuclear translocator [ARNT]) is an important member of the HIF family of transcription factors. In the normoxic environment, α subunit proteins of the HIF family are inhibited by the action of proline hydroxylase and cannot function. In the hypoxic environment, the proline pathway is inhibited. HIF α subunits can combine with β subunits to form heterodimers that activate hypoxic transport elements to relieve hypoxia. When there is a lack of HIF β subunits in the body, the HIF-1 pathway is inhibited. Studies have shown that the activity of HIF-1 cannot be induced in ARNT-deficient cells (10) and that HIF-1 cannot be expressed under hypoxic conditions. HIF-1 α must dimerize with HIF-1 β to form a heterodimer to function as a transcription factor.

Over the past decade, there has been gradual recognition of the importance of the gut microbiota. The gut microbiota is now considered to be a human organ with unique functions (11–13) that are important to maintain the balance of the body. Previous reports have described some effects of the hypoxic environment of the plateau climate on intestinal microbes (14, 15). The acute low-oxygen environment of a plateau stresses the body. Excitation of the sympathetic nervous system increases, causing dilation of the intestinal submucosal arteries and veins; the hypoxia and ischemia cause damage to the gastrointestinal mucosa (16), including barrier dysfunction and increased intestinal mucosal permeability, which may lead to an imbalance of intestinal flora. After 30 days of intermittent exposure of rats to a simulated hypoxic environment at an altitude of 4,872.9 m, the number of aerobic bacteria in the intestine decreased significantly whereas the number of facultative anaerobic bacteria increased significantly (17, 18). Acute exposure to the low-oxygen environment of a plateau is also known to lead to a decrease of *Bifidobacteria* abundance in the intestinal tract and to an imbalance of intestinal flora, with the rate of imbalance increasing at higher altitudes (19).

There are no published studies that detail the relationship between the gut microbiota and HIF-1 β in a hypoxic environment. We aimed to explore the effects of hypoxic conditions on the host response and changes in levels of intestinal microbes by comparing peripheral hemogram, serum cytokine expression, and the structure and diversity of the gut microbiota in wild-type (WT) and knockout (KO) mice with myeloid HIF-1 β depletion in myelomonocytic cells.

RESULTS

Hif-1 β deletion in myeloid cells aggravated the hypoxic phenotype. The rate of *Hif-1 β* deletion efficiency in this mouse line is approximately 60% to 70%, as detected by reverse transcription-PCR (data not shown). We induced a hypoxic model in mice raised in a composite hypoxia chamber. Changes in body weight in the KO and WT groups following 14 days of hypoxic exposure are shown in Fig. 1B. Severely decreased body weight was observed in both groups after only 1 day of exposure to hypoxia, indicating that acute hypoxia had a significant impact on the body. After the first day, the decrease in body weight continued daily but was less dramatic, with no difference between the two groups in the first 3 days. From day 4, body weight began to increase with small fluctuations, suggesting that the mice were beginning to adjust and gradually adapt to the hypoxic environment. Persistent differences between the groups in body weight also began on day 4, with a significantly lower rate of weight recovery in the KO group than in the WT group (Fig. 1B).

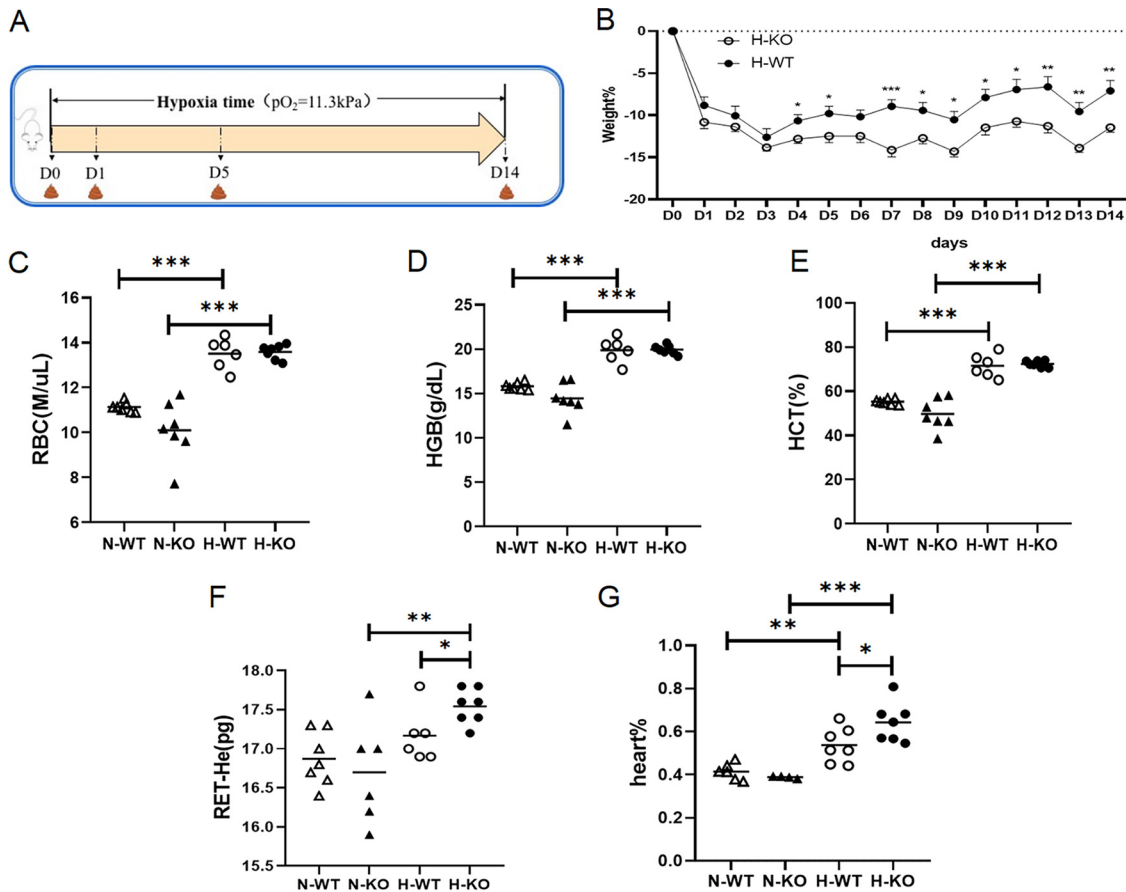


FIG 1 Hypoxic conditions resulted in weight loss, cardiac hypertrophy, and hematopoietic dysfunction in myeloid *Hif-1 β* -deficient mice. (A) Experimental design of microecological studies on myeloid *Hif-1 β* KO and WT mice under hypoxia conditions. The environment for induction of a hypoxia mouse model was a low-pressure hypoxia simulation cabin (simulated altitude, 5,000 m; oxygen partial pressure, 11.3 kPa). Fecal samples of mice were collected at 0, 1, 5, and 14 days after exposure to hypoxia. D0, day zero; D1, day 1; D5, day 5; D14, day 14. (B) Changes in body weight for mice in the *Hif-1 β* KO and WT groups in a hypoxic environment. (C to F) Comparison of erythrocyte parameters, including RBCs (C), HGB (D), HCT (E), and reticulocyte hemoglobin (RET-He) (F), between the *Hif-1 β* KO and WT groups in normoxic and hypoxic environments. (G) The heart-weight-to-body-weight ratio of the *Hif-1 β* KO model group and WT mice. Results are shown as means \pm SEM. N-WT, wild-type mice in normoxia environment; H-WT, wild-type mice in hypoxia environment; N-KO, knockout mice in normoxia environment; H-KO, knockout mice in hypoxia environment.

Hemogram data represent another important index used to measure hypoxia in animal models. The number of red blood cells (RBCs), level of hemoglobin (HGB), and percent hematocrit (HCT) were markedly higher in the mice raised in the hypoxic environment than in the mice raised in the normoxic environment (Fig. 1C to E), but no differences were found between the groups of WT and KO mice in the hypoxic environment (HWT and HKO groups, respectively). For leukocytes, there was no difference between the hypoxia and normoxia groups (see Fig. S1 in the supplemental material). Reticulocyte hemoglobin levels showed a difference between these two groups (Fig. 1F), indicating that the KO mice were more sensitive to hypoxia. Since hypoxia can lead to compensatory cardiac hypertrophy, we tested the heart index and found significant increases in mice raised in the hypoxic environment. The increases in heart index values were significantly higher in the HKO group than in the HWT group (Fig. 1G). Testing these groups for lung indices, we found no significant changes (Fig. S2). Pathological sectioning and hematoxylin and eosin (HE) staining of colon, heart, and lung were done, but no difference was found between the WT and KO groups (Fig. S3). Taken together, these results confirmed that the hypoxia mouse model was successfully established and that mice with the *Hif-1 β* deletion in myeloid cells displayed an obviously aggravated hypoxic phenotype.

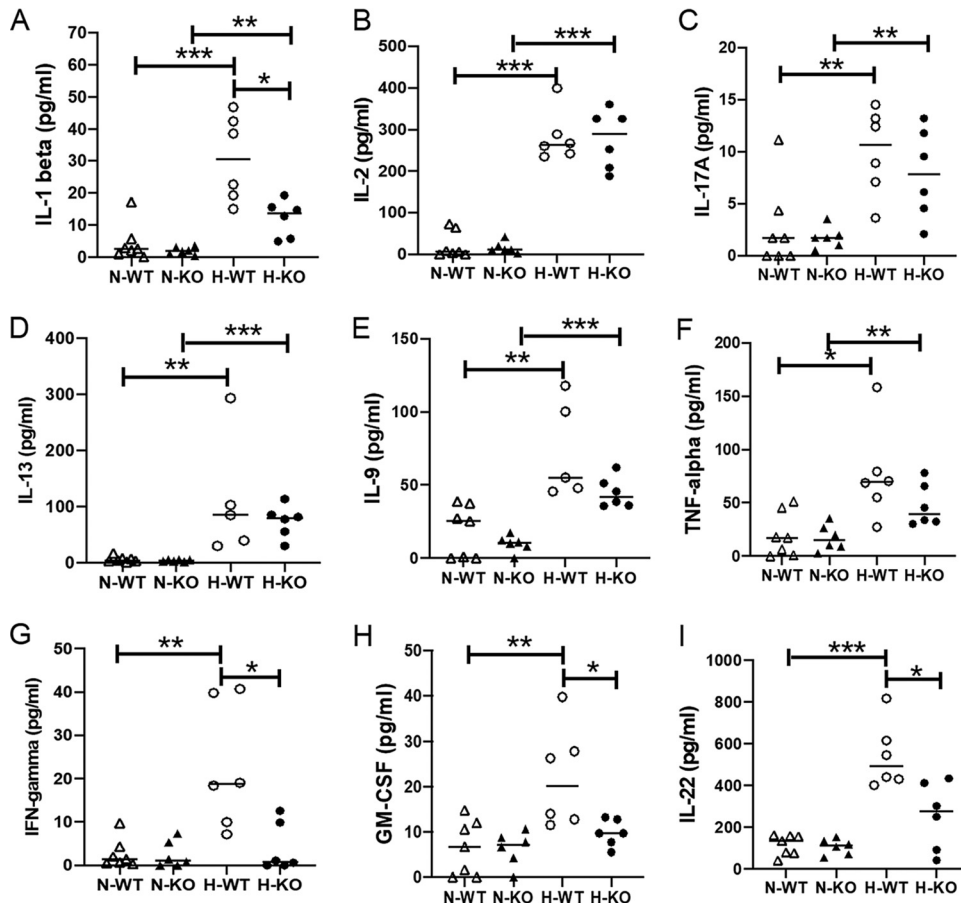


FIG 2 Comparison of serum levels of cytokines, including IL-1 beta (A), IL-2 (B), IL-17A (C), IL-13 (D), IL-9 (E), TNF-alpha (F), IFN gamma (G), GM-CSF (H), IL-22 (I), in the myeloid *Hif-1β* KO group and WT group under normoxic and hypoxic conditions. Results are shown as means \pm SEM.

Effects of hypoxia and *Hif-1β* deletion on cytokine secretion. Studies have shown that hypoxia increases the levels of proinflammatory cytokines such as tumor necrosis factor alpha (TNF- α), interleukin-1 β (IL-1 β), and IL-6 in human and animal plasma (20, 21). To study the effect of *Hif-1β* deletion in myeloid cells on cytokines under conditions of hypoxic stimulation, we examined the serum levels of several cytokines that are mainly secreted by myeloid cells. We detected significantly higher levels of IL-1 β , IL-2, IL-17A, IL-13, IL-9, and TNF- α in the hypoxic mice than in those in the normoxic environment (Fig. 2A to F). Levels of three cytokines (IL-4, IL-5, and IL-6) were significantly higher in the hypoxic environment than in the normoxic environment, but only in the WT groups; there was no significant change in these cytokines in the KO groups (Fig. S4A to C). Levels of IL-23 were higher only in the HWT group (Fig. S4D). On the basis of these results, we concluded that hypoxia increases the secretion of some cytokines in mice.

Further, we wanted to determine the effects of *Hif-1β* deletion in myeloid cells on cytokines. In the hypoxic environment, serum expression of IL-1 β , gamma interferon (IFN- γ), granulocyte-macrophage colony-stimulating factor (GM-CSF), and IL-22 showed significant differences between the HWT and HKO groups (Fig. 2A and G to I). The concentrations of these four cytokines were obviously higher in the HWT groups than in the HKO groups. For IL-1 β , hypoxia increased the level of secretion but myeloid *Hif-1β* deletion partly slowed its rapid rise. Increases in the levels of IFN- γ , GM-CSF, and IL-22 were found only in the HWT groups, which meant that *Hif-1β* took part in the regulation of myeloid cell function in the hypoxia environment. In addition, not all of

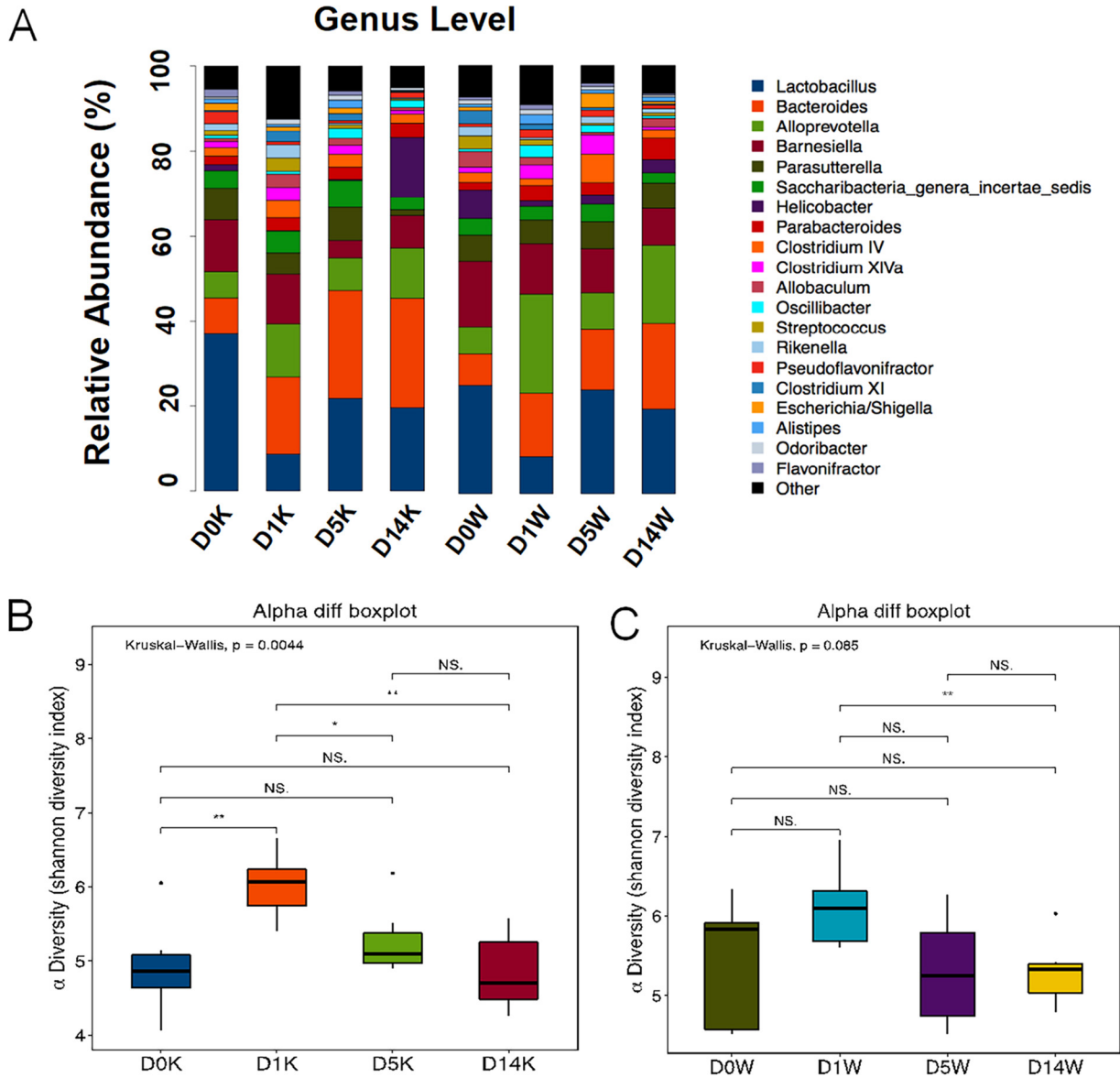


FIG 3 Microorganisms identified from the fecal samples in each group. (A) The relative abundances of the top 20 genera in the gut microbiota of all groups. (B and C) Shannon diversity indices of the KO group (B) and the WT group (C) at four time points. D0K, day zero knockout; D1K, day 1 knockout; D5K, day 5 knockout; D14K, day 14 knockout; D0W, day zero wild type; D1W, day 1 wild type; D5W, day 5 wild type; D14W, day 14 wild type.

the results seen with the cytokines affected by hypoxia, including IL-27, IL-18, IL-10, and IL-12 p70, were similar under normoxic and hypoxic conditions (Fig. S4E to H).

Hypoxia significantly changed the composition of the gut microbiota. The gut microbiota from the HKO and HWT groups were contrasted. In terms of the relative abundances of the top 20 genera on day 0 (Fig. 3A), *Lactobacillus*, *Bacteroides*, *Alloprevotella*, *Barnesiella*, *Parasutterella*, and *Helicobacter* dominated in the HWT group, with bacterial abundance of >6%. All but one (*Parasutterella*) of the same genera also showed bacterial abundance of >6% in the HKO group on day 0. After 1 day of hypoxia, there were obvious reductions in *Lactobacillus* abundance in both the HWT and HKO groups, indicating that *Lactobacillus* spp. are very sensitive to oxygen content. Because *Lactobacillus* is often regarded as a probiotic, the decrease in the abundance of this genus may have been one contributor to the dysbiosis. Furthermore, we noticed that *Lactobacillus* decreased in abundance by 16.67% in the WT group and by 28.26% in the

TABLE 1 Analysis of β -diversity by multiresponse permutation procedures^a

Group	Observed delta	Expected delta	P value
D0K_D1K_D5K_D14K	0.31821568	0.341490914	0.001
D0W_D1W_D5W_D14W	0.309877805	0.323862097	0.005
D0K_D0W	0.306147468	0.311721143	0.068
D1K_D1W	0.276883556	0.285851983	0.01
D5K_D5W	0.320061484	0.325940036	0.076
D14K_D14W	0.356954618	0.375684915	0.003

^aObserved delta, the observed delta values corresponding to the Unifrac distance index; Expected delta, the expected delta values corresponding to the Unifrac distance index.

KO group. After day 1, the composition of the gut microbiota gradually adjusted, but it was difficult to return the abundances to the original levels in the relatively short time frame. On the whole, the intestinal flora was greatly affected on the first day of hypoxia, which coincided with the sharp drop in body weight.

The Shannon diversity index revealed a change in bacterial diversity in the HKO group on the first day ($P = 0.0014$) and differences between day 1 and day 14 that were also statistically significant ($P = 0.017$) (Fig. 3B). In contrast, the variation in the HWT group on the first day was not as obvious as it had been in the HKO group, but the results were significantly different from the abundance measured at day 14 (Fig. 3C). The results of β -diversity analysis performed with multiresponse permutation procedures (MRPPs) to analyze intergroup differences showed that the UniFrac distance index value corresponding to the significance of the P value was <0.05 at four time points, indicating that obvious changes in the abundances of the intestinal microbes of mice had occurred during hypoxia (Table 1). Before hypoxia, there was no significant difference in the abundances of intestinal microorganisms between the HKO and HWT groups. On the first day of exposure to the hypoxic environment, the P value for β -diversity was <0.05 , indicating that the composition of the intestinal microbes fluctuated greatly when the mice first entered the hypoxia chamber, a determination that was supported by the α -diversity results.

Effect of *Hif1 β* deletion in myeloid cells on the gut microbiota in a hypoxic environment. To determine which species had a significant influence on the group division, a rank sum test was applied. The dynamic changes in the abundances of bacteria that differed from day 0 to day 14 are shown in Fig. 4. For most of the variant bacteria, the first day of hypoxia produced a significant change in abundance, followed by a gradual return to the abundance seen under normoxia conditions. Among all of the bacteria that showed a difference under hypoxia conditions, more than half appeared in both the HWT group (Fig. 4A) and the HKO group (Fig. 4B) and showed similar trends as indicated by the blue circles in Fig. 4. Examples of this phenomenon included the abundances of Bacilli at the class level and Lactobacillales at the order level, which all decreased dramatically at day 1 and then increased. These results demonstrated that hypoxia was clearly involved in regulating the gut microbiota. Other variant bacteria were found in only one group, and the variations may have been related to the gene KO. Abundances of *Bacteroidaceae* at the family level and *Bacteroides* at the genus level increased continuously in the HKO group.

Linear discriminant analysis (LDA) effect size (LEfSe) determinations were used to analyze differences in the intestinal microbial communities between the KO and WT groups at the indicated time points (Fig. 5). The results showed that on the first day of hypoxia (Fig. 5A), the distinct taxa in the HKO group were the family *Anaeroplasmataceae*, order *Anaeroplasmatales*, genus *Anaeroplasma*, class *Mollicutes*, phylum *Tenericutes*, genus *Enterorhabdus*, genus *Ruminococcus*, genus *Clostridium* cluster XVIII, genus *Odoribacter*, and phylum *Proteobacteria*, but only genus *Turicibacter* was unique to the HWT group. On day 5, the species that had a significant impact on sample division were found only in the KO group (Fig. 5B). At the end of the experiment, additional species that differed between the groups were detected (Fig. 5C). In summary, hypoxia-induced changes in intestinal microorganisms were more obvious in the HKO mice than in the HWT mice.

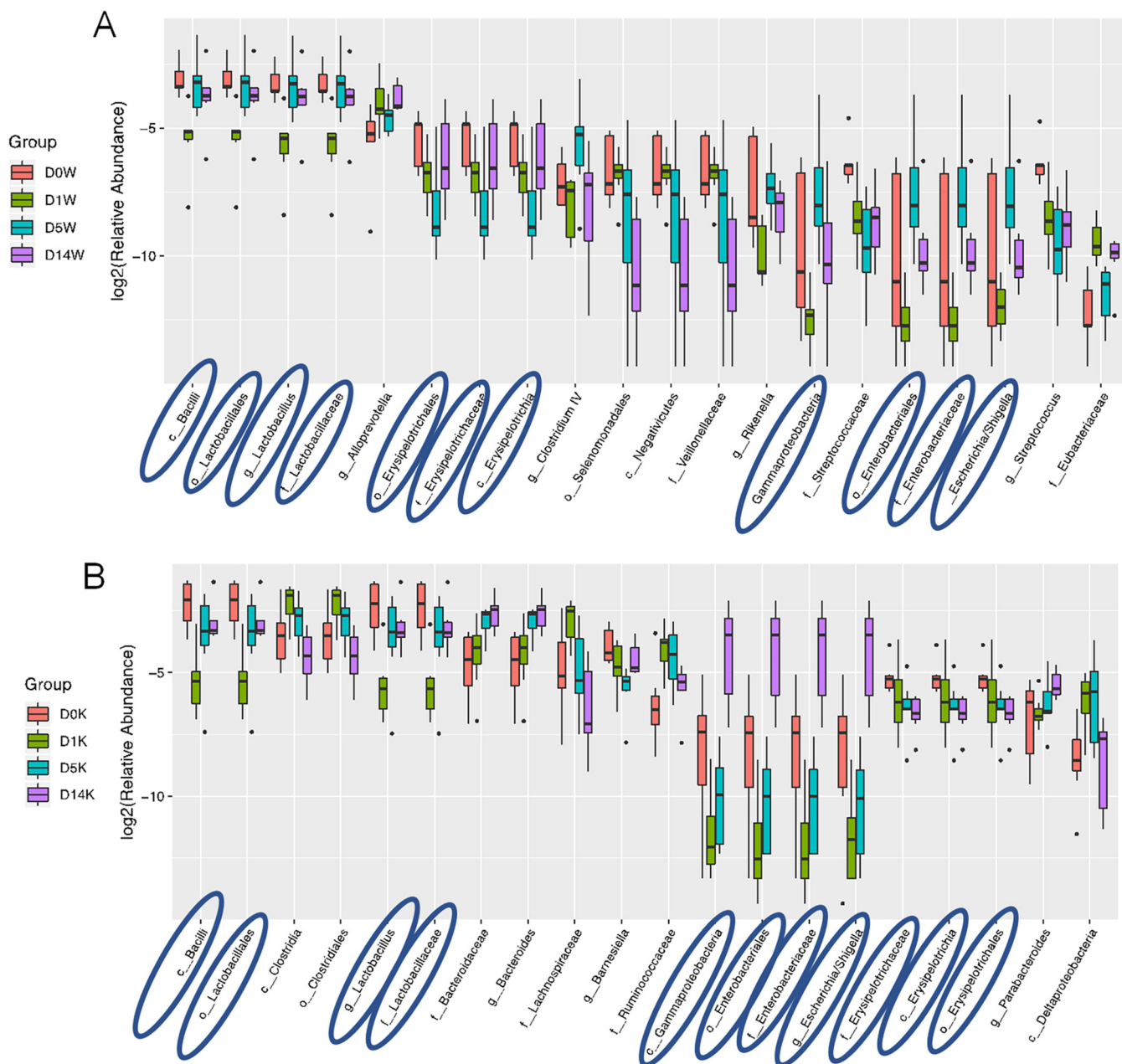


FIG 4 Boxplot display of genus-level differences in microbial species. Analysis of the significant differences was performed at the genus level in the top 20 microbes of the KO group (A) and WT group (B) at four time points. The bacteria in the blue ellipses represent those that appeared in both groups.

DISCUSSION

Plateau environments are characterized mainly by low pressure, hypoxia, and strong radiation. Hypoxia is one of the main causes of altitude sickness. It has been reported that people who move to a plateau from a plain environment experience obvious weight loss (22–24). Exposure to the hypoxia and hypobaric environment present at high altitudes leads to loss of appetite, reduction of food intake (22), increase of energy consumption (25), disturbance of gastrointestinal nutrient absorption function (23), and changes in basal metabolic rate (26). In this study, during the 14 days of hypoxia, the body weight of all mice initially decreased rapidly and then entered a stage of slow fluctuation and small increases as the body adapted to hypoxia. However, a significant difference in body weight between the HKO and HWT groups remained at the end of the experiment. In a state of hypoxia, the body secretes more erythropoietin to

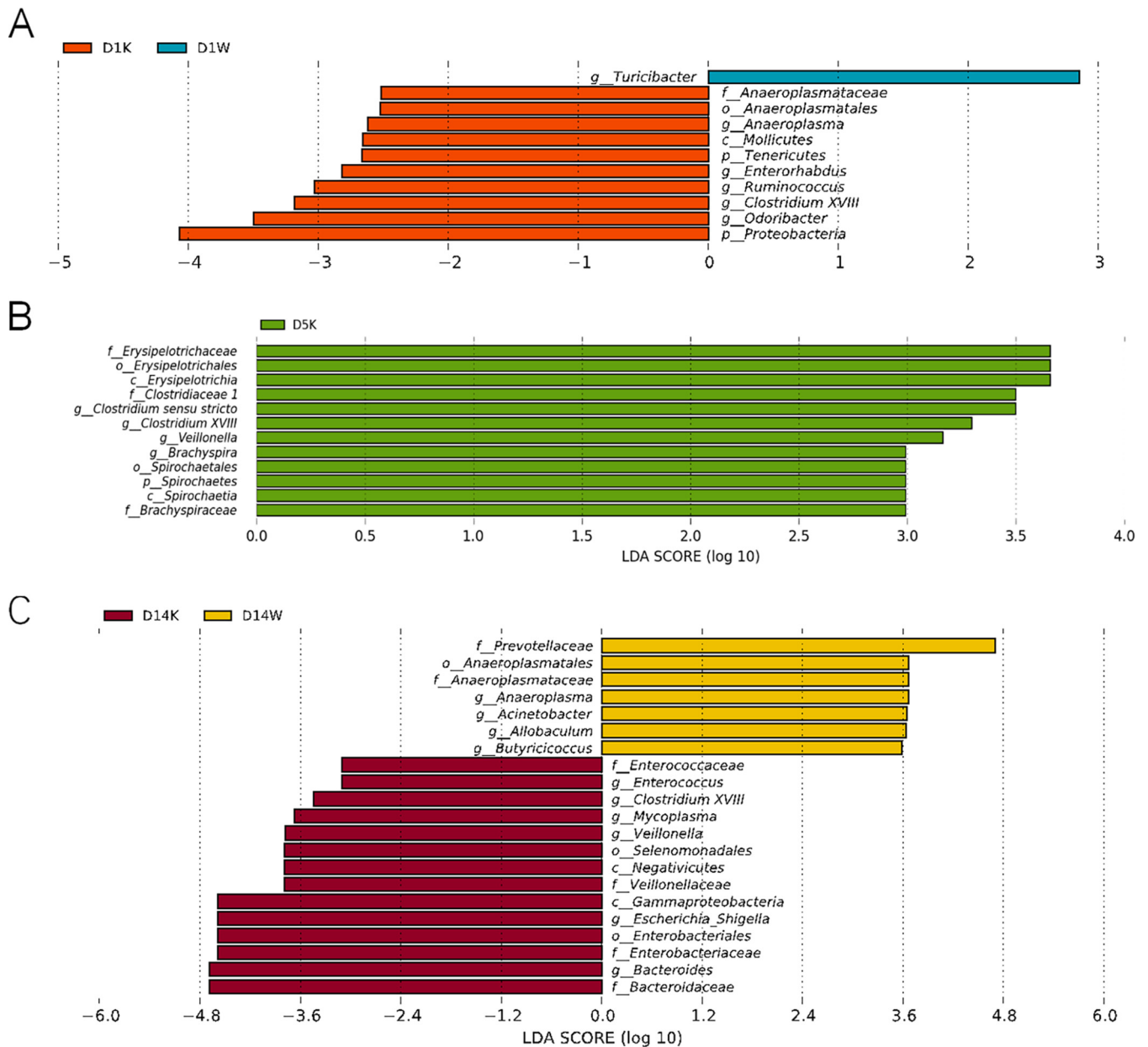


FIG 5 LDA effect size of microorganisms identified from each stool sample in mice in a low-oxygen environment. The figure shows the LDA score obtained by statistically analyzing the microbial groups with significant effects in different groups using linear regression analysis; different colors indicate different microbial groups. (A) LDA scores of microbial groups with significant effects on the KO and WT groups on day 1 of hypoxia. (B) LDA score of fecal microorganisms on day 5 of hypoxia in the KO group. (C) LDA scores of microbial groups with significant effects on the KO and WT groups on day 14.

synthesize hemoglobin, improving the oxygen-carrying capacity of the blood and thus improving tissue support. Indeed, we observed a significant increase in erythrocyte parameters in mice under hypoxia conditions.

Previous studies have shown that hypoxia activates inflammatory cells (monocytes/macrophages, neutrophils, and dendritic cells), which are further induced to secrete inflammatory cytokines (27). Therefore, we tested serum levels of 17 mouse cytokines in both the normoxic and hypoxic groups. The levels of TNF- α and IL-1 β were significantly higher in the hypoxic groups than in the normoxic groups, which is consistent with previous studies (28, 29). We noticed that the serum IL-1 β level in mice carrying a *Hif-1 β* deletion in myeloid cells was significantly lower than that in WT mice under hypoxic conditions. IL-1 β is produced and secreted mainly by monocytes/

macrophages and plays an immunomodulatory role locally. Its presence can accelerate migration of neutrophils to inflammatory sites to release oxidative stressors such as free radicals, lipid metabolites, and lysosomes (30). Some studies have shown that, after specific KO of the *Hif-1 α* gene in myeloid cells, they lose the ability to mount an inflammatory response, including migration, chemotaxis, aggregation, invasiveness, and bactericidal ability, and that the severity of the related inflammatory damage is also alleviated (31). In our study, IL-1 β , IFN- γ , GM-CSF, and IL-22 also showed significant decreases in the HKO group compared with the HWT group. Thus, under hypoxia conditions, the *Hif-1 β* deletion in myeloid cells reduced inflammatory response ability and diminished the serum levels of some cytokines.

Few studies have examined the effects of hypoxia on the gut microbiota (17, 32), even in humans (33, 34). Briefly, those studies suggested that high-altitude expeditions are associated with increased abundance of proinflammatory taxa, while associations with potentially beneficial taxa are inconsistent. We wondered what might be the effects of *Hif-1 β* gene deletion on intestinal microorganisms in a hypoxic environment. First, most of the species showing significantly different effects were seen in the KO group, meaning that the absence of *Hif-1 β* under low-oxygen conditions had a significant impact on intestinal microorganisms. Second, abundances of several specific bacterial species were found to be related to *Hif-1 β* under hypoxia conditions. The abundances of *Bacteroidaceae* at the family level and *Bacteroides* at the genus level increased constantly in the HKO group from day 1 to day 14, and they were the most obviously differentiated bacteria present at day 14 compared with the HWT group. The intestinal flora encompasses an extremely diverse microbial community, with about 500 species of bacteria in each individual (35), among which the *Bacteroidetes* are the most abundant and varied (36). A previous study showed that there were significant differences between a group maintained in a plateau environment and a group maintained in a plain environment in *Bacteroides* at the genus level (37). In this study, *Bacteroidetes* were found to be more abundant in *Hif-1 β* deletion mice than in WT mice in a hypoxic environment, which suggested that *Bacteroidetes* not only were sensitive to oxygen content but also might be able to sense changes in oxygen-related genes. However, such changes do not necessarily reflect a direct cause-and-effect relationship. In comparison to *Bacteroidetes*, Enterobacteriales at the order level and Gammaproteobacteria at the class level showed a different change. In HWT mice, these bacteria returned to nearly normal abundance at day 14, but in HKO mice, they showed even higher abundance at day 14. The right balance of locations, numbers, and species of bacteria is key to maintaining homeostasis in the gut. Overgrowth of *Enterobacter* spp. is conducive to bacterial translocation (38), which leads to the diffusion of endotoxins (39). Under hypoxia conditions, the WT mice showed better regulation of the gut microbiota than the KO mice in our study, which may partly explain the phenotypic differences between the two groups.

We found the presence of *Butyricoccus*, which are butyrate-producing bacteria, in the WT group after 14 days in the hypoxic environment, compared with the KO group. Butyrate-producing bacteria are beneficial bacteria that regulate the microecological balance of the human intestinal tract, which can promote the proliferation and development of beneficial intestinal flora, inhibit the growth and reproduction of harmful and putrid bacteria, correct disorders of intestinal flora, and reduce the secretion of enterotoxins (40, 41). Taking the results together, under low-oxygen conditions, the *Hif-1 β* deletion in myeloid cells affected the composition of the gut microbiota and slowed its reversion to a normal condition.

Simulation of the harsh hypoxic environment that is experienced on a plateau led to a series of changes in mice that resulted in intestinal flora imbalance and cytokine infiltration. The KO of *Hif-1 β* in myeloid cells worsened the clinical phenotypes and significantly altered the intestinal microbiota, which was reflected by gut microbiota composition and the abundance of some bacteria. Further study is necessary to explore the mechanism of the *Hif-1 β* -mediated response to hypoxia and to characterize the *Hif-1 β* -related microecological regulation strategy.

MATERIALS AND METHODS

Animals. All experiments were performed under specific-pathogen-free conditions in conformity with ethical guidelines and were approved by the Institutional Animal Care and Use Committee of the Medical Ethical Committee, Academy of Military Sciences (no. SCXK-2019-01070274). Myeloid-specific HIF-1 β -deficient (*Hif-1* $\beta^{fl/fl,lysM-cre+}$) KO mice on a C57BL/6 background were generated using the Cre-loxP recombination system (42). Briefly, *Hif1* $\beta^{lox/lox}$ mice (on the B6 genetic background) were crossed with *Lyz-cre* mice to obtain KO (*Hif-1* $\beta^{fl/fl,lysM-cre+}$) mice, and *Hif-1* $\beta^{fl/fl,lysM-cre-}$ mice were used for the WT group.

Study groups. Female mice aged 8 to 10 weeks and weighing 23 ± 3 g were divided into four groups ($n = 6$ to 7 mice/group) with the following designations: NKO (normoxia *Hif-1* $\beta^{fl/fl,lysM-cre+}$) mice, NWT (normoxia *Hif-1* $\beta^{fl/fl,lysM-cre-}$) mice, HKO (hypoxia *Hif-1* $\beta^{fl/fl,lysM-cre+}$) mice, and HWT (hypoxia *Hif-1* $\beta^{fl/fl,lysM-cre-}$) mice. The experimental cycle was 14 days. Mice in the hypoxia groups were exposed to a hypoxic environment (partial O₂ pressure [pO₂] = 11.3 kPa) for 20 h and to a normoxic environment (pO₂ = 21.1 kPa) for 4 h/day. The mice in the hypoxia groups were raised in a composite hypoxia chamber (Guizhou Fenglei Ltd., Guizhou, China), and the normoxia groups were raised in the Experimental Animal Center of the Beijing Institute of Microbiology and Epidemiology. The experimental design is shown in Fig. 1A. All utensils and feeds were sterilized. During the experiments, the animals were housed under a 12-h light/dark cycle at 18 to 22°C, their bedding was kept dry, and they were free to eat and drink water.

Blood and tissue sample collection. Blood was collected and divided into two parts. One part was analyzed by the use of an automatic hematology analyzer (IDEXX ProCyte DX; Edwards Biotechnology Co., Ltd., USA), and the other was separated by centrifugation to obtain serum for cytokine analysis. Colons were collected for formalin fixation. Hearts and lungs were weighed and subjected to formalin fixation prior to histology.

Detection of cytokine secretion. Serum was collected and assayed on high-throughput liquid protein chips (Luminex 200, USA). We used a mouse Th1/Th2/Th9/Th17/Th22/Treg cytokine panel (17-plex) kit (EPX170-26087-901; Thermo Fisher Scientific, USA) to detect expression of the following 17 cytokines: gamma interferon (IFN- γ), interleukin-12p70 (IL-12p70), IL-13, IL-1 β , IL-2, IL-4, IL-5, IL-6, tumor necrosis factor alpha (TNF- α), granulocyte-macrophage colony-stimulating factor (GM-CSF), IL-18, IL-10, IL-17A, IL-22, IL-23, IL-27, and IL-9.

Fecal sample collection. Fresh fecal samples were collected at the indicated times (Fig. 1A) and quickly transferred to a -80°C cryogenic freezer. The fecal samples were named according to their collection day (D) and genetic origin (K for KO; W for WT) as follows: D0K, D1K, D5K, D14K, D0W, D1W, D5W, and D14W. The collected stool samples were then subjected to DNA extraction for PCR.

Fecal microbiome analysis. (i) DNA extraction and PCR amplification. DNA was extracted from stool samples by the use of a TIANamp stool DNA minikit (Tiangen, Beijing, China) following the manufacturer's instructions. DNA concentration and purity were monitored on 1% agarose gels. The V3-V4 region of the 16S rRNA gene was amplified from the fecal DNA samples by the use of the following primer pair (43): 341F (5'-CCT ACG GGR SGC AGC AG-3') and 806R (5'-GGA CTA CVV GGG TAT CTA ATC-3'). All PCRs were carried out using a Kapa HiFi HotStart ReadyMix PCR kit (Annoron, Beijing, China).

(ii) PCR amplification and product purification. Using the diluted genomic DNA as the template, a Kapa HiFi HotStart ReadyMix PCR kit (Annoron, Beijing, China) was used for PCR to ensure the accuracy and efficiency of amplification. PCR products were detected after separation by electrophoresis in a 2% agarose gel, and the PCR products were recovered using an AxyPrep DNA gel recovery kit (Axygen, CA, USA). After recovery, a Thermo NanoDrop 2000 ultraviolet microspectrophotometer and 2% agarose gel electrophoresis were used to perform quality control of the library.

Sequencing analysis. The 16S rRNA sequencing data were optimized and statistically analyzed using PANDAseq software (44). Next, we performed an operational taxonomic unit (OTU) cluster analysis by sorting the clean reads with the same sequence, filtering to obtain the species-level classification, and then comparing all clean reads with the OTU sequence to extract the corresponding read sequence for the final mapped reads.

The most abundant sequence in each OTU is its representative sequence, which can be compared with the sequences in the 16S database of known species (RDP; <http://rdp.cme.msu.edu>) and ultimately classified for each OTU species. Each sample is classified with respect to the sequence number at each level of species classification (i.e., phylum, class, order, family, genus, and species) to gain an overall picture at each level (45, 46). The results of species classification can be mapped to a corresponding histogram so that the relative abundances and proportions of species can be viewed intuitively based on the different taxonomic levels (phylum, class, order, family, genus, and species) for each sample (47).

α -Diversity mainly refers to the diversity of a specific region or a single sample, and the α -diversity index is a comprehensive index used to reflect richness and evenness. We used QIIME software (48, 49) to calculate the value of the α -diversity index for a single sample and to draw the corresponding α -diversity curve. The α -diversity curve is used to calculate the expected value of the α -diversity index by extracting n (where n is less than the total number of measured read sequences) from the relative proportions of all types of known 16S rRNA gene OTU sequences. The curve is then drawn using a group of n values (generally an isometric series comprising less than the total sequence number) and the corresponding expected values, and a statistical α -diversity index table is generated (50). The Shannon index can be used to comprehensively assess the richness and evenness of a community; the higher the

Shannon index value, the higher the diversity. The formula to calculate the Shannon index is as follows:

$$H_{\text{Shannon}} = - \sum_{i=1}^{\text{Sobs}} \frac{n_i}{N} \ln \frac{n_i}{N}$$

Unlike α -diversity analysis, β -diversity analysis is used to compare the levels of species diversity among samples. To assess the structural similarity of intestinal microflora between KO mice and WT mice, a multiresponse permutation procedure (MRPP) analysis based on Unifrac distance matrix was used. MRPP analysis, similarly to analysis of similarity (ANOSIM), is a statistical method used to analyze similarities between high-dimensional data (51).

Taxonomic linear discriminant analysis (LDA) effect size (LEfSe) determinations focus on identifying communities or species that have a significant impact on the division of a sample under different grouping conditions. LEfSe data emphasize statistical significance, biological consistency, and effect correlation (45).

Statistical analysis. Data are presented as means \pm standard errors of the means (SEM). Comparisons of means were performed using the Student's *t* test contained within the GraphPad Prism 8.0 program. Differences between groups were considered significant at *P* values of <0.05 .

SUPPLEMENTAL MATERIAL

Supplemental material is available online only.

SUPPLEMENTAL FILE 1, PDF file, 0.1 MB.

SUPPLEMENTAL FILE 2, PDF file, 0.1 MB.

SUPPLEMENTAL FILE 3, PDF file, 1.7 MB.

SUPPLEMENTAL FILE 4, PDF file, 0.1 MB.

ACKNOWLEDGMENTS

This research was supported by the National Natural Science Foundation of China (grant no. 31970863), the National Natural Science Foundation for Key Programs of China (grant no. 81790632), and the Innovation Leader Team Program of Guangzhou (no. 201809010014). We thank Michelle Kahmeyer-Gabbe of Liwen Bianji, Edanz Editing China (www.liwenbianji.cn/ac), for editing the English text of a draft of the manuscript.

Consent for publication is not applicable.

All of the data that were generated and analyzed in this study are included in this published article (or its supplemental material files).

We declare no competing interests.

N.H. did the experiments, analyzed the data, and wrote the manuscript. Z.P. and Z.H. did the experiments and analyzed the data. Y.C. and F.H. investigated the literature and analyzed the data. R.Y. provided the overall direction for the experiments. G.L. provided mice and designed the experiments. Y.B. designed the experiments, analyzed the data, provided the overall direction, and contributed to manuscript revisions.

REFERENCES

- Huerta-Sanchez E, Jin X, Asan Bianba Z, Peter BM, Vinckenbosch N, Liang Y, Yi X, He M, Somel M, Ni P, Wang B, Ou X, Huasang Luosang J, Cuo ZX, Li K, Gao G, Yin Y, Wang W, Zhang X, Xu X, Yang H, Li Y, Wang J, Wang J, Nielsen R. 2014. Altitude adaptation in Tibetans caused by introgression of Denisovan-like DNA. *Nature* 512:194–197. <https://doi.org/10.1038/nature13408>.
- Mejia OM, Prchal JT, Leon-Velarde F, Hurtado A, Stockton DW. 2005. Genetic association analysis of chronic mountain sickness in an Andean high-altitude population. *Haematologica* 90:13–19.
- Vargas E, Spielvogel H. 2006. Chronic mountain sickness, optimal hemoglobin, and heart disease. *High Alt Med Biol* 7:138–149. <https://doi.org/10.1089/ham.2006.7.138>.
- Beall CM, Cavalleri GL, Deng L, Elston RC, Gao Y, Knight J, Li C, Li JC, Liang Y, McCormack M, Montgomery HE, Pan H, Robbins PA, Shianna KV, Tam SC, Tsering N, Veeramah KR, Wang W, Wangdui P, Weale ME, Xu Y, Xu Z, Yang L, Zaman MJ, Zeng C, Zhang L, Zhang X, Zhaxi P, Zheng YT. 2010. Natural selection on EPAS1 (HIF2 α) associated with low hemoglobin concentration in Tibetan highlanders. *Proc Natl Acad Sci U S A* 107: 11459–11464. <https://doi.org/10.1073/pnas.1002443107>.
- Horscroft JA, Kotwica AO, Laner V, West JA, Hennis PJ, Levett DZH, Howard DJ, Fernandez BO, Burgess SL, Ament Z, Gilbert-Kawai ET, Vercueil A, Landis BD, Mitchell K, Mythen MG, Branco C, Johnson RS, Feilisch M, Montgomery HE, Griffin JL, Grocott MPW, Gnaiger E, Martin DS, Murray AJ. 2017. Metabolic basis to Sherpa altitude adaptation. *Proc Natl Acad Sci U S A* 114:6382–6387. <https://doi.org/10.1073/pnas.1700527114>.
- Leon-Velarde F, Maggiorini M, Reeves JT, Aldashev A, Asmus I, Bernardi L, Ge RL, Hackett P, Kobayashi T, Moore LG, Penaloza D, Richalet JP, Roach R, Wu T, Vargas E, Zubieta-Castillo G, Zubieta-Calleja G. 2005. Consensus statement on chronic and subacute high altitude diseases. *High Alt Med Biol* 6:147–157. <https://doi.org/10.1089/ham.2005.6.147>.
- Peacock AJ. 1998. ABC of oxygen: oxygen at high altitude. *BMJ* 317: 1063–1066. <https://doi.org/10.1136/bmj.317.7165.1063>.
- Koh MY, Powis G. 2012. Passing the baton: the HIF switch. *Trends Biochem Sci* 37:364–372. <https://doi.org/10.1016/j.tibs.2012.06.004>.
- Hede K. 2004. Environmental protection: studies highlight importance of tumor microenvironment. *J Natl Cancer Inst* 96:1120–1121. <https://doi.org/10.1093/jnci/96.15.1120>.
- Chakraborty AA, Laukka T, Myllykoski M, Ringel AE, Booker MA, Tolstorukov MY, Meng YJ, Meier SR, Jennings RB, Creech AL, Herbert ZT, McBrayer SK, Olenchok BA, Jaffe JD, Haigis MC, Beroukhim R, Signoretti S, Koivunen P, Kaelin WG, Jr. 2019. Histone demethylase KDM6A directly senses oxygen to control chromatin and cell fate. *Science* 363: 1217–1222. <https://doi.org/10.1126/science.aaw1026>.
- Marietta E, Horwath I, Balakrishnan B, Taneja V. 2019. Role of the intestinal microbiome in autoimmune diseases and its use in treatments. *Cell Immunol* 339:50–58. <https://doi.org/10.1016/j.cellimm.2018.10.005>.
- Desai MS, Seekatz AM, Koropatkin NM, Kamada N, Hickey CA, Wolter M,

- Pudlo NA, Kitamoto S, Terrapon N, Muller A, Young VB, Henrissat B, Wilmes P, Stappenbeck TS, Nunez G, Martens EC. 2016. A dietary fiber-deprived gut microbiota degrades the colonic mucus barrier and enhances pathogen susceptibility. *Cell* 167:1339–1353.e21. <https://doi.org/10.1016/j.cell.2016.10.043>.
13. Shepherd ES, DeLoache WC, Pruss KM, Whitaker WR, Sonnenburg JL. 2018. An exclusive metabolic niche enables strain engraftment in the gut microbiota. *Nature* 557:434–438. <https://doi.org/10.1038/s41586-018-0092-4>.
 14. Kleessen B, Schroedel W, Stueck M, Richter A, Rieck O, Krueger M. 2005. Microbial and immunological responses relative to high-altitude exposure in mountaineers. *Med Sci Sports Exerc* 37:1313–1318. <https://doi.org/10.1249/01.mss.0000174888.22930.e0>.
 15. Facco M, Zilli C, Siviero M, Ermolao A, Travain G, Baesso I, Bonamico S, Cabrelle A, Zaccaria M, Agostini C. 2005. Modulation of immune response by the acute and chronic exposure to high altitude. *Med Sci Sports Exerc* 37:768–774. <https://doi.org/10.1249/01.mss.0000162688.54089.ce>.
 16. Sridharan K, Ranganathan S, Mukherjee AK, Kumria ML, Vats P. 2004. Vitamin status of high altitude (3660 m) acclimatized human subjects during consumption of tinned rations. *Wilderness Environ Med* 15: 95–101. [https://doi.org/10.1580/1080-6032\(2004\)015\[0095:vsosham\]2.0.co;2](https://doi.org/10.1580/1080-6032(2004)015[0095:vsosham]2.0.co;2).
 17. Adak A, Maity C, Ghosh K, Mondal KC. 2014. Alteration of predominant gastrointestinal flora and oxidative damage of large intestine under simulated hypobaric hypoxia. *Z Gastroenterol* 52:180–186. <https://doi.org/10.1055/s-0033-1336007>.
 18. Adak A, Ghosh, Mondal KC. 2014. Modulation of small intestinal homeostasis along with its microflora during acclimatization at simulated hypobaric hypoxia. *Indian J Exp Biol* 52:1098–1105.
 19. Lei F, JWJWCJoD J. 2010. Influence of Bifidobacterium on the intestinal microflora and corticotropin-releasing factor in rats following chronic psychological stress. *World Chin J Digestol* 18:1544–1549. (In Chinese.) <https://doi.org/10.11569/wcjdv.18.i15.1544>.
 20. Spielmann S, Kerner T, Ahlers O, Keh D, Gerlach M, Gerlach H. 2001. Early detection of increased tumour necrosis factor alpha (TNFalpha) and soluble TNF receptor protein plasma levels after trauma reveals associations with the clinical course. *Acta Anaesthesiol Scand* 45:364–370. <https://doi.org/10.1034/j.1399-6576.2001.045003364.x>.
 21. Wu SQ, Aird WC. 2005. Thrombin, TNF-alpha, and LPS exert overlapping but nonidentical effects on gene expression in endothelial cells and vascular smooth muscle cells. *Am J Physiol Heart Circ Physiol* 289: H873–H885. <https://doi.org/10.1152/ajpheart.00993.2004>.
 22. Rose MS, Houston CS, Fulco CS, Coates G, Sutton JR, Cymerman A. 1988. Operation Everest. II: nutrition and body composition. *J Appl Physiol* (1985) 65:2545–2551. <https://doi.org/10.1152/jappl.1988.65.6.2545>.
 23. Boyer SJ, Blume FD. 1984. Weight loss and changes in body composition at high altitude. *J Appl Physiol Respir Environ Exerc Physiol* 57: 1580–1585. <https://doi.org/10.1152/jappl.1984.57.5.1580>.
 24. Kayser B. 1994. Nutrition and energetics of exercise at altitude. Theory and possible practical implications. *Sports Med* 17:309–323. <https://doi.org/10.2165/00007256-199417050-00004>.
 25. Westerterp KR, Brouns F, Saris WH, ten Hoor F. 1988. Comparison of doubly labeled water with respirometry at low- and high-activity levels. *J Appl Physiol* (1985) 65:53–56. <https://doi.org/10.1152/jappl.1988.65.1.53>.
 26. Hamad N, Travis SP. 2006. Weight loss at high altitude: pathophysiology and practical implications. *Eur J Gastroenterol Hepatol* 18:5–10. <https://doi.org/10.1097/00042737-200601000-00002>.
 27. Ferhani N, Letuve S, Kozhich A, Thibaudeau O, Grandsaigne M, Maret M, Dombret MC, Sims GP, Kolbeck R, Coyle AJ, Aubier M, Pretolani M. 2010. Expression of high-mobility group box 1 and of receptor for advanced glycation end products in chronic obstructive pulmonary disease. *Am J Respir Crit Care Med* 181:917–927. <https://doi.org/10.1164/rccm.200903-0340OC>.
 28. Pintus G, Tadolini B, Posadino AM, Sanna B, Debidda M, Carru C, Deiana L, Ventura C. 2003. PKC/Raf/MEK/ERK signaling pathway modulates native-LDL-induced E2F-1 gene expression and endothelial cell proliferation. *Cardiovasc Res* 59:934–944. [https://doi.org/10.1016/s0008-6363\(03\)00526-1](https://doi.org/10.1016/s0008-6363(03)00526-1).
 29. Jeong HJ, Hong SH, Park RK, Shin T, An NH, Kim HM. 2005. Hypoxia-induced IL-6 production is associated with activation of MAP kinase, HIF-1, and NF-kappaB on HEI-OC1 cells. *Hear Res* 207:59–67. <https://doi.org/10.1016/j.heares.2005.04.003>.
 30. Patwari PP, O’Cain P, Goodman DM, Smith M, Krushkal J, Liu C, Somes G, Quasney MW, Dahmer MK. 2008. Interleukin-1 receptor antagonist intron 2 variable number of tandem repeats polymorphism and respiratory failure in children with community-acquired pneumonia. *Pediatr Crit Care Med* 9:553–559. <https://doi.org/10.1097/PCC.0b013e31818d32f1>.
 31. Cramer T, Yamanishi Y, Clausen BE, Forster I, Pawlinski R, Mackman N, Haase VH, Jaenisch R, Corr M, Nizet V, Firestein GS, Gerber HP, Ferrara N, Johnson RS. 2003. HIF-1alpha is essential for myeloid cell-mediated inflammation. *Cell* 112:645–657. [https://doi.org/10.1016/s0092-8674\(03\)00154-5](https://doi.org/10.1016/s0092-8674(03)00154-5).
 32. Xu CL, Sun R, Qiao XJ, Xu CC, Shang XY, Niu WN. 2014. Protective effect of glutamine on intestinal injury and bacterial community in rats exposed to hypobaric hypoxia environment. *World J Gastroenterol* 20: 4662–4674. <https://doi.org/10.3748/wjg.v20.i16.4662>.
 33. Sket R, Debevec T, Kublik S, Schloter M, Schoeller A, Murovec B, Vogel Mikus K, Makuc D, Pecnik K, Plavec J, Mekjavic IB, Eiken O, Prevorsek Z, Stres B. 2018. Intestinal metagenomes and metabolomes in healthy young males: inactivity and hypoxia generated negative physiological symptoms precede microbial dysbiosis. *Front Physiol* 9:198. <https://doi.org/10.3389/fphys.2018.00198>.
 34. Sket R, Treichel N, Debevec T, Eiken O, Mekjavic I, Schloter M, Vital M, Chandler J, Tiedje JM, Murovec B, Prevorsek Z, Stres B. 2017. Hypoxia and inactivity related physiological changes (constipation, inflammation) are not reflected at the level of gut metabolites and butyrate producing microbial community: The PlanHab Study. *Front Physiol* 8:250. <https://doi.org/10.3389/fphys.2017.00250>.
 35. Backhed F, Ley RE, Sonnenburg JL, Peterson DA, Gordon JI. 2005. Host-bacterial mutualism in the human intestine. *Science* 307: 1915–1920. <https://doi.org/10.1126/science.1104816>.
 36. Tap J, Mondot S, Levenez F, Pelletier E, Caron C, Furet JP, Ugarte E, Munoz-Tamayo R, Paslier DL, Nalin R, Dore J, Leclerc M. 2009. Towards the human intestinal microbiota phylogenetic core. *Environ Microbiol* 11:2574–2584. <https://doi.org/10.1111/j.1462-2920.2009.01982.x>.
 37. Sun Y, Zhang J, Zhao A, Li W, Feng Q, Wang R. 2020. Effects of intestinal flora on the pharmacokinetics and pharmacodynamics of aspirin in high-altitude hypoxia. *PLoS One* 15:e0230197. <https://doi.org/10.1371/journal.pone.0230197>.
 38. Berg RD. 1995. Bacterial translocation from the gastrointestinal tract. *Trends Microbiol* 3:149–154. [https://doi.org/10.1016/s0966-842x\(00\)88906-4](https://doi.org/10.1016/s0966-842x(00)88906-4).
 39. Wang XD, Soltész V, Andersson R. 1996. Cisapride prevents enteric bacterial overgrowth and translocation by improvement of intestinal motility in rats with acute liver failure. *Eur Surg Res* 28:402–412. <https://doi.org/10.1159/000129484>.
 40. Hamer HW, Jonkers D, Venema K, Vanhoutvin S, Troost FJ, Brummer RJ. 2008. Review article: the role of butyrate on colonic function. *Aliment Pharmacol Ther* 27:104–119. <https://doi.org/10.1111/j.1365-2036.2007.03562.x>.
 41. Louis P, Hold GL, Flint HJ. 2014. The gut microbiota, bacterial metabolites and colorectal cancer. *Nat Rev Microbiol* 12:661–672. <https://doi.org/10.1038/nrmicro3344>.
 42. Clausen BE, Burkhardt C, Reith W, Renkawitz R, Forster I. 1999. Conditional gene targeting in macrophages and granulocytes using LysMcre mice. *Transgenic Res* 8:265–277. <https://doi.org/10.1023/a:1008942828960>.
 43. Thijs S, Op De Beeck M, Beckers B, Truysens S, Stevens V, Van Hamme JD, Weyens N, Vangronsveld J. 2017. Comparative evaluation of four bacteria-specific primer pairs for 16S rRNA gene surveys. *Front Microbiol* 8:494. <https://doi.org/10.3389/fmicb.2017.00494>.
 44. Masella AP, Bartram AK, Truszowski JM, Brown DG, Neufeld JD. 2012. PANDAseq: paired-end assembler for Illumina sequences. *BMC Bioinformatics* 13:31. <https://doi.org/10.1186/1471-2105-13-31>.
 45. Segata N, Izard J, Waldron L, Gevers D, Miropolsky L, Garrett WS, Huttenhower C. 2011. Metagenomic biomarker discovery and explanation. *Genome Biol* 12:R60. <https://doi.org/10.1186/gb-2011-12-6-r60>.
 46. Wang Y, Qian PY. 2009. Conservative fragments in bacterial 16S rRNA genes and primer design for 16S ribosomal DNA amplicons in metagenomic studies. *PLoS One* 4:e7401. <https://doi.org/10.1371/journal.pone.0007401>.
 47. Bellemain E, Carlsen T, Brochmann C, Coissac E, Taberlet P, Kausserud H. 2010. ITS as an environmental DNA barcode for fungi: an in silico

- approach reveals potential PCR biases. *BMC Microbiol* 10:189. <https://doi.org/10.1186/1471-2180-10-189>.
48. Caporaso JG, Kuczynski J, Stombaugh J, Bittinger K, Bushman FD, Costello EK, Fierer N, Pena AG, Goodrich JK, Gordon JI, Huttley GA, Kelley ST, Knights D, Koenig JE, Ley RE, Lozupone CA, McDonald D, Muegge BD, Pirrung M, Reeder J, Sevinsky JR, Turnbaugh PJ, Walters WA, Widmann J, Yatsunenko T, Zaneveld J, Knight R. 2010. QIIME allows analysis of high-throughput community sequencing data. *Nat Methods* 7:335–336. <https://doi.org/10.1038/nmeth.f.303>.
49. Kemp PF, Aller JY. 2004. Bacterial diversity in aquatic and other environments: what 16S rDNA libraries can tell us. *FEMS Microbiol Ecol* 47:161–177. [https://doi.org/10.1016/S0168-6496\(03\)00257-5](https://doi.org/10.1016/S0168-6496(03)00257-5).
50. Yu Z, Yang J, Liu L, Zhang W, Amalfitano S. 2015. Bacterioplankton community shifts associated with epipelagic and mesopelagic waters in the Southern Ocean. *Sci Rep* 5:12897. <https://doi.org/10.1038/srep12897>.
51. Galimanas V, Hall MW, Singh N, Lynch MD, Goldberg M, Tenenbaum H, Cvitkovitch DG, Neufeld JD, Senadheera DB. 2014. Bacterial community composition of chronic periodontitis and novel oral sampling sites for detecting disease indicators. *Microbiome* 2:32. <https://doi.org/10.1186/2049-2618-2-32>.